Generation of Elliptically Polarized Terahertz Waves from Laser-Induced Plasma with Double Helix Electrodes

Xiaofei Lu and X.-C. Zhang

Phys. Rev. Lett. **108**, 123903 — Published 21 March 2012

DOI: 10.1103/PhysRevLett.108.123903

Generation of Elliptically Polarized Terahertz Waves from Laser-Induced Plasma with Double Helix Electrodes

Xiaofei Lu and X.-C. Zhang*

Department of Physics, Applied Physics, and Astronomy, Center for Terahertz Research, Rensselaer Polytechnic Institute, Troy, New York 12180, USA

PACS: 42.65.Re, 52.50.Jm, 32.80.Fb

Abstract

By applying a helical electrical field along plasma region, a revolving electron current is formed along plasma and an elliptically polarized far-field terahertz wave pattern is observed. The observed terahertz wave polarization reveals the remarkable role of velocity retardation between optical pulses and generated terahertz pulses in the generation process. Extensive simulations, including longitudinal propagation effects, are performed to clarify the mechanisms responsible for polarization control of air-plasma based terahertz sources.

* Email: zhangxc@rpi.edu

Electromagnetic pulses in the terahertz (THz) frequency range play a pivotal role in material spectroscopy, biomedical diagnosis and homeland security.[1] However, coherently exciting and controlling a circular polarized THz wave has proved to be a challenge, primarily because most pulsed THz sources are based on optical rectification[2] or transient dipole radiation.[3] Elliptically or circularly polarized THz waves are potentially important to study macromolecular chiral structures such as proteins and DNA or excite spin dynamics in solid state materials. Typically, a Fresnel prism is used as a quarter wave plate for THz waves to switch linear polarization to circular polarization.[4] The introduced material absorption and Fresnel loss limit the bandwidth and intensity of THz waves. The latest advances in plasma based THz sources[5-12] have made it possible to observe and even control linear polarization state of intense and broadband THz waves through a coherent manipulation of the motion of ionized electron electrically[7, 12] or optically.[13-14] In all these experiments, the trajectory of released electrons, which contribute to the THz polarization state, is determined by the direction of the external field or the relative phase of two-colored optical fields. Although an imperfection of THz polarization state such as elliptical polarization from these plasma sources has been reported,[13, 15] insightful physical and theoretical explanation are required for further polarization control and manipulation.

In this letter, we present a combined theoretical and experimental study of elliptical polarization properties of generated THz waves from a laser-induced plasma with a pair of double helix electrodes. We demonstrate that temporal propagation effects are indispensable for

understanding the THz wave generation process and influence the THz polarization substantially. In both experiments and simulations, we observe a remarkable properties change of the elliptical THz polarization state with various electrodes design. Such ellipticity is a result of a sensitive dependence of the velocity mismatch between propagation of the optical pulses and generated THz pulses. Extensive numerical simulations were performed combining transient current model with pulse velocity retardation, which includes the longitudinal propagation effects responsible for polarization control of THz waves.

In the laser-induced ionization process, electrons released from molecules or atoms exhibit a net drifting current after passage of the laser pulses when they experience an asymmetric electrical field.[10-11, 16] This drifting current, which contributes to the far-field THz radiation, is aligned with the direction of an external DC field[12, 15] or asymmetric optical field.[13-14] In our experiment with a pair of double helix electrodes, during the travel of the ionization front, which associates with the propagation of intense laser pulses, the induced net electron current is revolving along the filament due to the longitudinal variation of applied DC electrical field. Furthermore, due to the velocity mismatch between THz wave and optical beam, we find that the produced THz wave will travel ahead of optical excitation, which will eventually lead to a phase difference between the produced s and p components of THz pulse in the far field due to the retarded radiation. We demonstrate that the THz polarization state can be coherently manipulated by varying the electrode design and longitudinal properties of plasma. For example, the

handedness can be controlled directly through the control of handedness of electrodes and the ellipticity can be controlled by electrodes design.

A Ti-sapphire amplified laser system, which can deliver laser pulses of 40 fs and 3 mJ at a repetition rate of 1 kHz, is used in this experiment. The laser pulses were split into pump beam and probe beam by a 95% to 5% beam splitter. The optical pump beam was focused by a lens with 400 mm focal length to produce an ionization region with more than 40 mm length in air. **Fig. 1** shows the illustration of revolving electrical field and a laboratory coordinate. A pair of double helix electrodes, which is made from two copper wires with a 1 mm diameter, was mounted along the plasma region. The two copper wires were twisted for only one period along the grooves on a plastic mount, which has an inner diameter of 4 mm and an outer diameter of 6 mm. The inter spacing is around 5 mm and the length of one pitch is 30 mm. The pitch length was chosen to optimize the elipticity of produced THz waves under current experimental condition. The bias field was provided by a high voltage modulator, which delivers bipolar square waves with a frequency of 500 Hz and a tunable amplitude up to 3 kV. The generated THz wave was collected by a 90˚ off-axis parabolic mirror and then focused again by another parabolic mirror. A 1 mm thick high resistivity silicon wafer was inserted between two parabolic mirrors to block the residue optical beam. The optical probe beam went through a time delay stage and then was focused by a lens with 150 mm focal length through a hole on second parabolic mirror onto a 1 mm thick (110) ZnTe crystal to resolve the temporal information of THz waves. To analyze the polarization of THz waves, a wired grid THz polarizer was used in

the collimated THz beam path. A combination of a half wave plate and a polarizer was inserted into the optical pump and probe beam to rotate the polarization of the pump and probe beams. The **Fig. 1** also provides the information about our laboratory coordinate. The x and y axis represent p and s polarizations, respectively. Note that the applied electrical field originates along the x-axis in laboratory coordinate and revolves clockwise or anti-clockwise depending on the handedness.

In order to clarify the effect related to pump beam polarization, we performed initial measurements by rotating the polarization of pump beam using a half wave plate, which is not shown here. The variation of the peak-to-peak amplitude of the p component of THz radiation is independent on pump beam polarization, which is also confirmed in Ref[15].

An elliptically polarized wave can be resolved into an arbitrary set of mutually orthogonal component waves with their polarization perpendicular to each other and with a fixed phase change. By recomposing the THz electric fields obtained at two orthogonal directions, it is feasible to derive the elliptical trajectories if the THz pulse is elliptically polarized. In our experiment, the polarization of THz waves was obtained by composing the THz electric fields in two orthogonal directions measured by electro-optic sampling technique, which is shown in **Fig. 2**. An elliptical THz polarization trajectory with an ellipticity e=0.5 was observed on X-Y plane in **Fig. 2(a)** and **(b)**. In the presence of the external helical electrical field, the handedness of elliptically polarized THz waves can be manipulated by the longitudinally revolving the direction

of DC field. A THz wave generated from a pair of linear electrodes is also shown in **Fig. 2 (c)** for comparison.

A theoretical model was built to explain all observed phenomenon. When applying an external bias field on plasma, the driven motion of electrons inside plasma will result in a far-field THz radiation, whose polarization is aligned to the external electrical field direction. The plasma can be described by electron density $\rho(t)$, which satisfies $\frac{\partial \rho(t)}{\partial t} = W_{ST}(t)(\rho_0 - \rho(t))$, where ρ_0 is the molecular gas density. $W_{ST}(t)$ is the ionization rate calculated from static tunneling model, which can be written as $W_{ST}(t) = \frac{\alpha}{\hat{E}_\omega(t)} \exp\left(-\frac{\beta}{\hat{E}_\omega(t)}\right)$,[17] where $\hat{E}_\omega(t) = E_\omega(t)/E_a$ is the electrical field of fundamental beam in atomic units, $E_a = m^2 e^5 / (4\pi\varepsilon_0)^3 \hbar^4$, $\alpha = 4\omega_a r_H^{5/2}$, $\beta = 2r_H^{3/2}/3$, $\omega_a = me^4/(4\pi\varepsilon_0)^2\hbar^3$, and $r_H = U/U_H$ is the relative molecular ionization potential normalized with that of hydrogen. m, e is the electron mass and charge, respectively. Here, the direction of applied electrical field is alternating along the plasma, which can be expressed as: $\vec{E}_{DC}(z) = E_0 \cos(\gamma z)\vec{x} \pm E_0 \sin(\gamma z)\vec{y}$, where E_0 is the amplitude of electrical field, $\gamma = 2\pi / L$ is the alternating frequency which is related to the pitch length of electrodes L, the sign of second term is determined by the handedness. Considering the averaged collision time of electron with ion τ , $\vec{v}(z,t,t_0) = -\frac{e}{m}\int_{t_0}^{t} [\vec{E}_{DC}(z) + \vec{E}_\omega(z,t')]H(t'-\tau)dt'$ shows the velocity of electrons born at time $t = t_0$, where $H(t'-\tau)$ is the Heaviside function used to describe electron collision.[11]

The transient current which corresponding to THz radiation is

$$\vec{J}(z,t) = e\int_{-\infty}^{t} \vec{v}(z,t,t_0)\dot{\rho}(t_0)dt_0 \qquad (1)$$

We used the retarded solution for one-dimensional Maxwell equation

$$\vec{A}(t) = \frac{\mu_0}{4\pi R} \int \vec{J}(z,t) e^{ik_{THz}(R-z)} dz \tag{2}$$

to describe the longitudinal propagation effect on far-field THz radiation pattern. $\vec{A}(t)$ is the vector potential for THz waves, μ_0 is the vacuum permeability, R is the distance from origin to field point position, $k_{THz} = \Omega / v_{THz}$ is the wave number, Ω is the angular frequency of THz waves and v_{THz} is the speed of THz waves in air .

The constructed far-field THz radiation is

$$\vec{E}_{THz}(t) \propto \frac{e^{ik_{THz}R}}{R} \int_{-L/2}^{L/2} \frac{\partial \vec{J}(z, t - k_{opt} z/\omega)}{\partial t} e^{-ik_{THz}z} dz \tag{3}$$

where $t - k_{opt} z/\omega$ describes the propagation of optical pulses in air.

In Eq. (3), obviously, the mismatch between k_{opt} and k_{THz} will contribute to the vector properties of far-field THz radiation. We modeled the dynamic process under our experimental condition by considering a focused Gaussian beam, whose peak value along z-axis can be expressed as $E_\omega(z,t) = E_\omega \frac{w_0}{w(z)} \exp(-2t^2/\tau_0^2)$. $w(z) = w_0[1 + (\lambda z/\pi w_0^2)^2]^{1/2}$ represents the optical field distribution along z axis , w_0 is the beam waist, and λ is the wavelength.

In our experiment, we estimated this velocity mismatch by measuring the time delay between two detected THz waves generated at the beginning and the end of the plasma and the corresponding difference in index of refraction is $\Delta n = n_{opt} - n_{THz} = 1.08 \times 10^{-4}$ which is used in all our simulations. Moreover, we ignore the individual air dispersion effect for optical pulses or THz pulses and only consider the relative dispersion between them. By considering the pulse duration and the focusing condition of laser beams, we estimated the power density in focus

region to be 10^{15} W/cm^2 and the induced plasma density to be within the range of 10^{15} cm^{-3}~ 10^{16} cm^{-3}, assuming the focal spot with a diameter of 100 um. Due to the velocity mismatch between optical pulses and THz pulses during propagation, within the coherent length, the constructed far-field radiation shows the arbitrary elliptical polarization. The simulated results for various electrodes are shown in **Fig. 2(d), (e)** and **(f)** for comparison. The simulated results agree well with experimental findings and also, depending on the revolving direction of electrical field, the polarization of output THz pulse demonstrates a controllable handedness.

Moreover, one interesting phenomenon is related to longitudinal symmetry of plasma density and the pitch length of applied electrical field. We noted that as we move the electrodes away from the center of the plasma, the constructed far-field THz radiation shows different ellipticity. To demonstrate the effects associated with plasma profile, **Fig. 3 (a)** and **(b)** shows a series of measured x and y components of THz field while moving electrodes position along plasma with right-handed and left-handed electrodes, respectively. A case with linear electrodes is also shown in **Fig. 3(c)** for comparison. The theoretical calculated results are also shown in **Fig. 3(d)**, **(e)** and **(f)** with corresponding condition of applied electrical field. The black curves reveal the polarization properties of far-field THz radiation at various positions, which defines as the relatively position between the centers of plasma and the electrodes. We found that, in our method, the property of far-field THz polarization depends not only with applied electrical field, but also with the uniformity of plasma.

To clarify elliptically polarized THz waves generated from double helix electrodes, we compared the results with that obtained by a Fresnel prism made of high-density polyethylene (HDPE). **Fig. 4(a)** and **(b)** plot the electric vector of right-handed and left-handed circularly polarized THz wave obtained with the Fresnel prism, respectively. The input THz polarization was controlled by a THz polarizer. Two main characters of circular or elliptical polarized beam are amplitude ratio E_x / E_y and phase difference $\varphi_x - \varphi_y$ between x and y components. For a perfect circularly polarized broadband pulses, $E_x(\omega) / E_y(\omega) = 1$ and $\varphi_x(\omega) - \varphi_y(\omega) = \pm\pi/2$ hold for all the frequencies. We extracted the amplitude ratio and the phase difference between x and y components through Fourier transform of experimental data and plotted in **Fig. 4(c)-(h)** for each case. Due to the large index of refraction and absorption of HDPE, the E_x / E_y and $\varphi_x - \varphi_y$ have a relatively large fluctuation around optimized number. As contrast, with double helix electrodes, especially at the position around the center of the plasma, the phase difference and amplitude ratio have minimum fluctuation across the spectral range, providing an elliptical polarized THz wave. This plasma based method, excluded from the alignment, absorption, and Fresnel loss issues, after further improvement with flexible design of electrodes, better controlled plasma profile and higher energy conversion efficiency, is a possible solution to provide an intense and broadband elliptically polarized terahertz wave.

To produce a nearly circularly polarized THz waves through our method, the plasma longitudinal profile and the electrode pitch length are two principle factors. From the above discussion, it is obvious that E_x / E_y of produced THz pulses is related to the plasma

longitudinal profile since the generation efficiency is consequentially associated to the plasma density, and $\varphi_x - \varphi_y$ is strongly dependent on the pitch length of the revolving electrical field since the phase difference is provided from the velocity mismatch. These two factors provide the design parameters of this plasma based circular polarized THz sources.

In conclusion, we demonstrate that the polarization of far-field THz radiation can be significantly modified through manipulation of revolving electron transient current in laser filament with a pair of double helix electrodes. An elliptically polarized far-field THz wave pattern is observed and demonstrated to be highly sensitive to the handedness of applied electrical field and position of electrodes. The velocity mismatch between optical excitation and propagation of THz waves is verified to be the mainly mechanism behind. This finding provides new perception of plasma-based THz emitters, opens interesting perspectives to coherently control polarization properties of THz emission in a broader spectral range and offers a useful diagnostics tool for biomolecular and spintronics study in THz frequency.

The authors would like to thank Dr. Jianming Dai for useful discussion. Xiaofei Lu is funded by the National Science Foundation IGERT Program under Grant No. 0333314. This work is supported in part by the National Science Foundation and the Defense Threat Reduction Agency.

Figure captions:

FIG. 1 (Color online) Illustration of double helix electrodes and corresponding electrical field applied on plasma region with different handedness. The laser pulses are focused to ionize air where a pair of double helix electrodes was positioned. The trajectory of electrons (blue arrows) follows the external electrical field direction, resulting in an elliptically polarized THz wave in the far field. The laboratory coordinate and definition of handedness are shown in the figure. The origin is defined at the center of the plasma.

FIG. 2 (Color online) Temporal evolution of electrical field vector of (a) right-handed and (b) left-handed elliptically polarized and (c) linear polarized THz pulses. Simulated temporal evolution of electrical field vector of (d) right-handed and (e) left-handed elliptically polarized and (f) linear polarized THz pulses. EXP: experimental results. SIM: simulation results.

FIG. 3 (Color online) The measured far-field THz waves in x (upper) and y (lower) direction at various electrodes position from pairs of (a) right-handed, (b) left-handed helical and (c) linear electrodes. The calculated far-field THz waves in x and y direction at various electrodes position from (d) right-handed and (e) left-handed helical and (f) linear electrodes are also shown for comparison. The red curves show the polarization trajectories of far-field THz radiation at position z=-20, -10, 0, 10 mm, respectively. EXP: experimental results. SIM: simulation results.

FIG. 4 (Color online) Measured temporal evolution of electrical field vector of (a) right-handed and (b) left-handed circular polarized THz pulses with a HDPE Fresnel prism. The phase difference and amplitude ratio between x and y component for (c) right-handed and (d)

left-handed circular polarized THz pulses in frequency domain. The (e) phase difference and (f) amplitude ratio of elliptically polarized THz pulses generated from double helix electrodes are shown for comparison. EXP: experimental results. SIM: simulation results.

References:

1. M. Tonouchi, Nat. Photonics **1**, 97 (2007).
2. B. B. Hu, X.-C. Zhang, D. H. Auston and P. R. Smith, Appl. Phys. Lett. **56**, 506 (1990).
3. G. Mourou, C. V. Stancampiano and D. Blumenthal, Appl. Phys. Lett. **38**, 470 (1981).
4. J. Shan, J. I. Dadap and T. F. Heinz, Opt. Express **17**, 7431 (2009).
5. H. Hamster, A. Sullivan, S. Gordon, W. White and R. W. Falcone, Phys. Rev. Lett. **71**, 2725 (1993).
6. D. J. Cook and R. M. Hochstrasser, Opt. Lett. **25**, 1210 (2000).
7. T. Loffler, F. Jacob and H. G. Roskos, Appl. Phys. Lett. **77**, 453 (2000).
8. T. Bartel, P. Gaal, K. Reimann, M. Woerner and T. Elsaesser, Opt. Lett. **30**, 2805 (2005).
9. M. Kress, T. Loffler, M. D. Thomson, R. Dorner, H. Gimpel, K. Zrost, T. Ergler, R. Moshammer, U. Morgner, J. Ullrich and H. G. Roskos, Nat. Phys. **2**, 327 (2006).
10. K. Y. Kim, J. H. Glownia, A. J. Taylor and G. Rodriguez, Opt. Express **15**, 4577 (2007).
11. M. D. Thomson, M. Kress, T. Loffler and H. G. Roskos, Laser Photonics Rev. **1**, 349 (2007).
12. A. Houard, Y. Liu, B. Prade, V. T. Tikhonchuk and A. Mysyrowicz, Phys. Rev. Lett. **100**, 255006 (2008).
13. J. Dai, N. Karpowicz and X.-C. Zhang, Phys. Rev. Lett. **103**, 023001 (2009).
14. H. Wen and A. M. Lindenberg, Phys. Rev. Lett. **103**, 023902 (2009).
15. Y. P. Chen, T. J. Wang, C. Marceau, F. Theberge, M. Chateauneuf, J. Dubois, O. Kosareva and S. L. Chin, Appl. Phys. Lett. **95**, 101101 (2009).
16. K. Y. Kim, A. J. Taylor, J. H. Glownia and G. Rodriguez, Nat. Photonics **2**, 605 (2008).
17. P. B. Corkum, N. H. Burnett and F. Brunel, Phys. Rev. Lett. **62**, 1259 (1989).

Figures

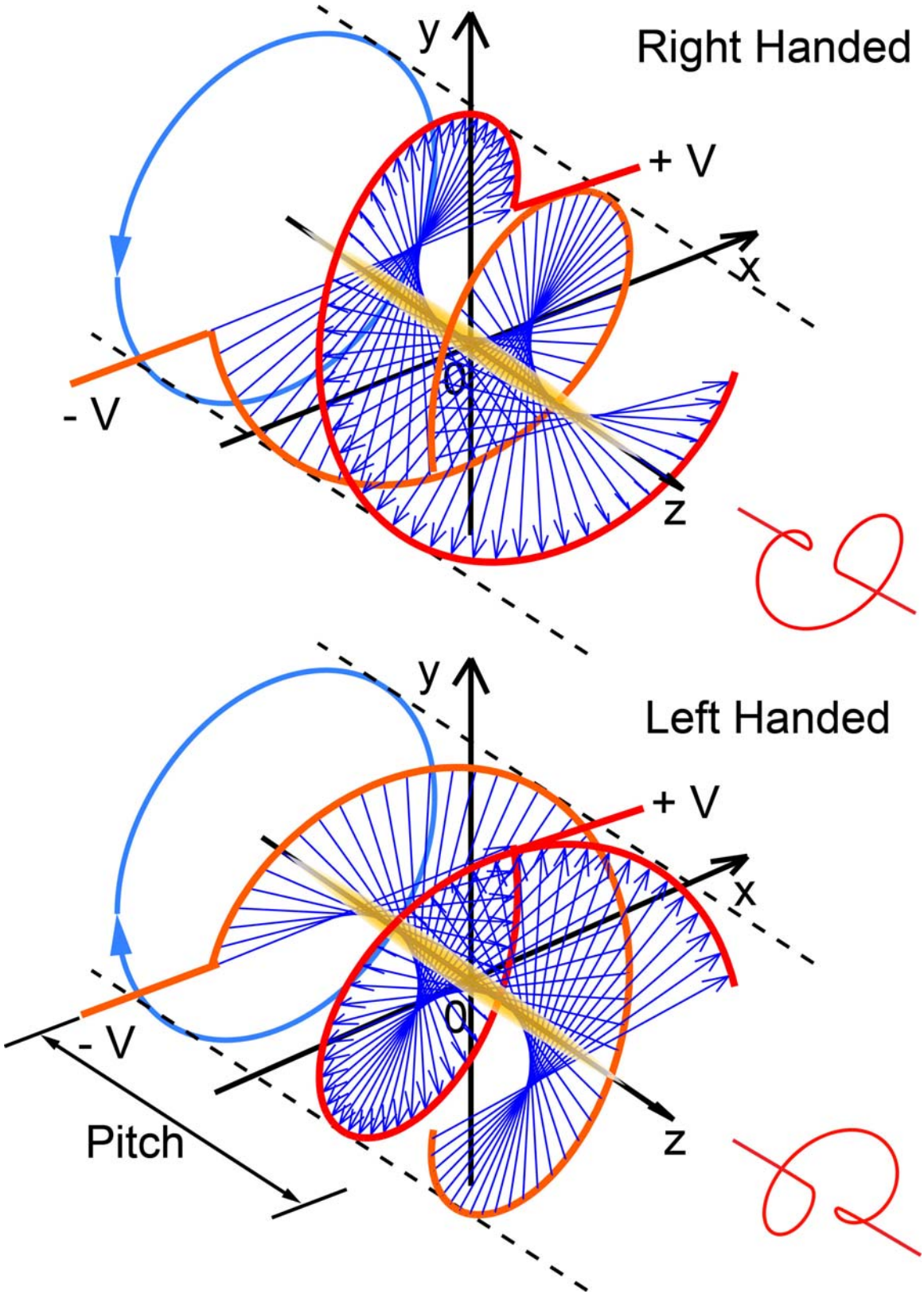

X. Lu et. al FIG. 1/4

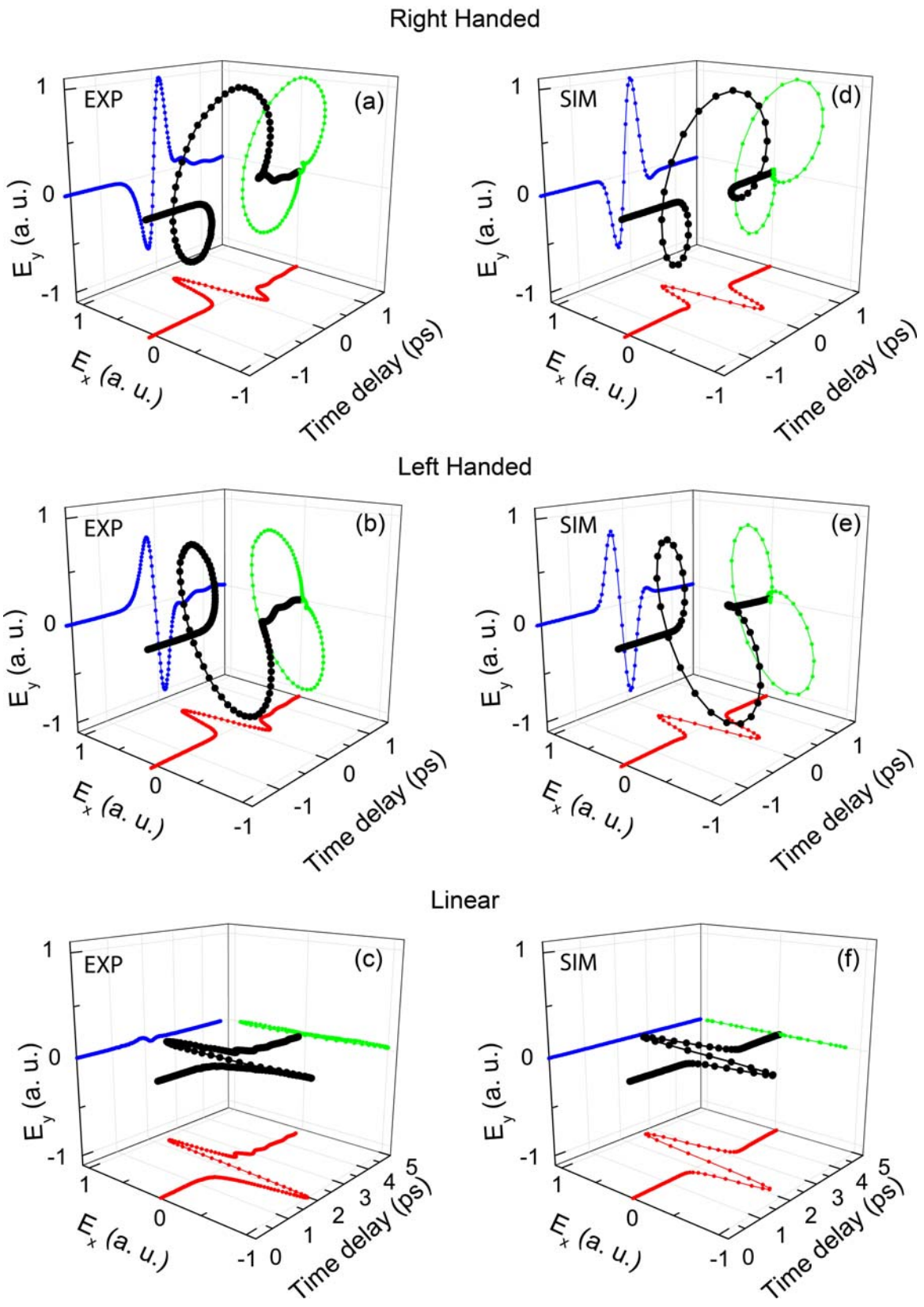

X. Lu et. al FIG. 2/4

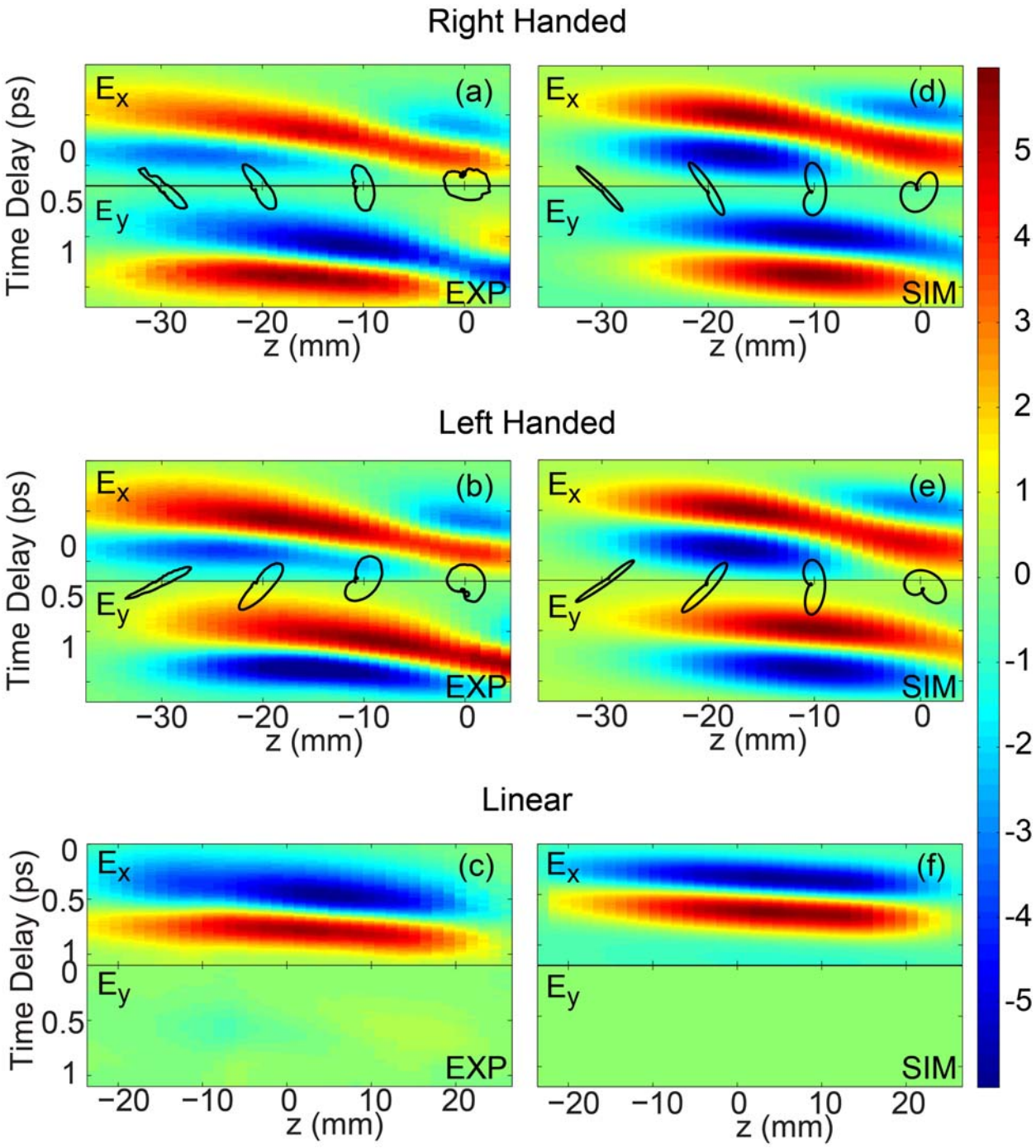

X. Lu et. al FIG. 3/4

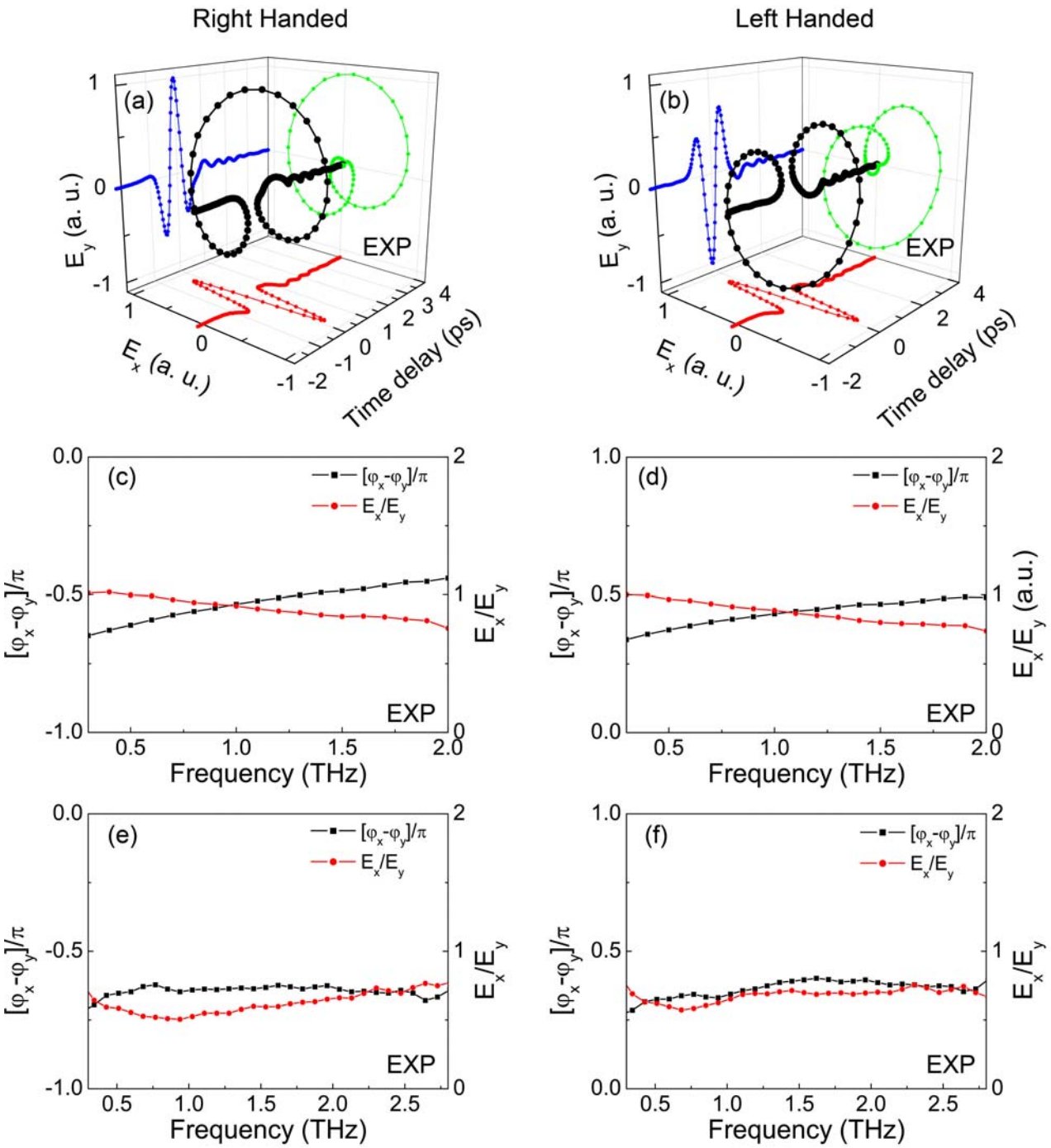

X. Lu et. al FIG. 4/4